Eriodictyol protects H9c2 cardiomyocytes against the injury induced by hypoxia/reoxygenation by improving the dysfunction of mitochondria

YANLI XIE[1], RONGWEI JI[2] and MINGHUI HAN[3]

[1]Department of Cardiothoracic Surgery, Wuhan Women and Children Medical Care Center, Wuhan, Hubei 430000; [2]Department of Pathology, Xi'an XD Group Hospital, Xi'an, Shaanxi 710077; [3]Department of Thoracic Surgery, The First People's Hospital of Qingdao Economic and Technological Development Zone, Qingdao, Shandong 266555, P.R. China

Received December 5, 2016; Accepted June 29, 2017

DOI: 10.3892/etm.2018.6918

Abstract. Myocardial infarction is a leading cause of mortality worldwide, while myocardial ischemia and timely reperfusion contribute to myocardial injury. The mitochondria are involved in the injury and mediate the apoptosis of cardiomyocytes. In order to develop novel therapeutic approaches for myocardial infarction, the present study evaluated the myocardial protective effects of eriodictyol and investigated relevant mechanisms in H9c2 cardiomyocytes. As a result, eriodictyol was observed to improve the H9c2 cardiomyocyte viability and block the leakage of cytosolic lactate dehydrogenase under hypoxia/reoxygenation. In addition, the dysfunction of mitochondria induced by hypoxia/reoxygenation was ameliorated by eriodictyol through suppressing the overload of intracellular Ca^{2+}, preventing overproduction of reactive oxygen species, blocking mitochondrial permeability transition pore opening, increasing mitochondrial membrane potential level and decreasing ATP depletion. Finally, the apoptosis of H9c2 cardiomyocyte induced by hypoxia/reoxygenation was prevented by eriodictyol through upregulation of the expression of B-cell lymphoma-2 (Bcl-2) and downregulation of the expression levels of Bcl-2-associated X protein and caspase-3. These results provided evidence for further investigation on myocardial protection and the treatment of myocardial infarction using eriodictyol.

Introduction

Myocardial infarction is a leading cause of mortality in humans worldwide, which results from myocardial ischemia (1,2). Timely reperfusion is considered as an effective therapy to limit the infarction size, although reperfusion of the ischemic myocardium will increase the number of patients with heart failure due to the cardiomyocyte death (3). The mitochondria are involved in the reperfusion injury, and the opening of mitochondrial permeability transition pore (MPTP) contributes to the infarction (4,5). In addition, intracellular Ca^{2+} overload and oxidative stress in mitochondria are also associated with myocardial infarction (6). In the development of effective therapeutic approaches for myocardial infarction, natural compounds serve an important role, including berberine (7), tanshinone IIA (8) and lycopene (9).

Eriodictyol (Fig. 1) is a flavonoid identified in numerous medicinal plants, such as *Bauhinia ungulata* (10), *Arcytophyllum thymifolium* (11), *Elsholtzia bodinieri* (12) and *Clinopodium chinense* (13). Pharmacological investigations have revealed that eriodictyol possesses several bioactivities, including neuroprotection (14-16), renoprotection (17) and lung protection (18), exerted via anti-inflammation and anti-oxidation. In addition, its anti-inflammatory and anti-oxidative capacities have drawn attention to its therapeutic potential (19-23).

With the aim to investigate bioactive phytochemicals for the treatment of myocardial infarction, the protective effects of eriodictyol on H9c2 cardiomyocyte injury induced by hypoxia/reoxygenation are investigated in the present study. The protective effect of eriodictyol is reported *in vitro*.

Materials and methods

Chemicals and reagents. Eriodictyol was purchased from YuanYe Biotechnology Co., Ltd. (Shanghai, China). Dulbecco's modified Eagle's medium (DMEM), fetal bovine serum (FBS) and calcein acetoxymethyl (calcein-AM) were obtained from Thermo Fisher Scientific, Inc. (Waltham, MA, USA). Dimethyl sulfoxide (DMSO) and 3-(4,5-dimethylthiazol-2-yl)-2,5-diphenyltetrazolium bromide (MTT) and were purchased from Sigma-Aldrich (Merck AG, Darmstadt, Germany). Reactive oxygen species (ROS), lactate dehydrogenase (LDH) and bicinchoninic acid (BCA) assay kits were supplied by Nanjing

Correspondence to: Dr Minghui Han, Department of Thoracic Surgery, The First People's Hospital of Qingdao Economic and Technological Development Zone, 9 Huangpu River Road, Qingdao, Shandong 266555, P.R. China
E-mail: medhanmh@126.com

Key words: eriodictyol, H9c2 cardiomyocyte, hypoxia/reoxygenation, mitochondrial dysfunction, myocardial protection

Jiancheng Bioengineering Institute (Nanjing, China). JC-1, Fluo-3 AM, ATP detection kit and caspase-3 assay kit, as well as cleaved caspase-3 (cat. no. AC033), B-cell lymphoma-2 (Bcl-2; cat. no. AB112), Bcl-2-associated X protein (Bax; cat. no. AB026) and actin (cat. no. AA128) antibodies (all 1:1,000) were purchased from Beyotime Institute of Biotechnology (Nantong, China).

Cell culture and treatment. The H9c2 cardiomyocytes, a rat embryonic cardiac myoblast line, were obtained from the Cell Bank of Chinese Academy of Sciences (Shanghai, China) and cultured as previously described (9). Briefly, H9c2 cells were cultured in DMEM containing 10% FBS and 1% penicillin/streptomycin under humid condition with 5% CO_2 and 95% air at 37˚C. Next, cells at the logarithmic phase were incubated in 96-well plates at a density of $1x10^5$/ml. The cells were then divided into the control group (CG), model group (MG) and three eriodictyol groups, which were pretreated with 1, 10 and 50 μM eriodictyol in DMSO for 4 h. In order to establish the hypoxia/reoxygenation model, H9c2 cells in the MG and eriodictyol groups were subjected to an atmosphere with 95% N_2 and 5% O_2 at 37˚C for 4 h, and then cultured under a condition of 95% air and 5% O_2 at 37˚C for a further 4 h. The CG cells were cultured under normoxic conditions.

Cell viability assay. To evaluate the protective effect of eriodictyol on the H9c2 cardiomyocyte injury induced by hypoxia/reoxygenation, an MTT assay was conducted. Following the aforementioned treatments, the cells were incubated with 0.2 ml MTT for 4 h at 37˚C. Subsequently, 200 μl DMSO was added into each well to dissolve the formazan crystals, and the absorbance was recorded on an iMark microplate reader (Bio-Rad Laboratories, Inc., Hercules, CA, USA) at 490 nm. The experiments were repeated three times.

Determination of LDH activity. The extracellular LDH activity was determined using the LDH assay kit, according to the manufacturer's instructions. Following treatment and incubation, the H9c2 cardiomyocyte culture medium was centrifuged at 400 x g and room temperature for 5 min, and then 20 μl supernatant was mixed with 20 μl 2,4-dinitrophenylhydrazine. The mixture was incubated at 37˚C for 15 min. Next, 250 μl NaOH (0.4 M) was added into the reaction system and incubated for a further 15 min at 37˚C. Subsequent to keeping at room temperature for 5 min, the absorbance was recorded on a microplate reader at 450 nm. The activity of LDH was calculated based on the absorbance as previously reported (24) and is expressed as U/l.

Detection of intracellular Ca^{2+}. In order to monitor the cytosolic Ca^{2+} content in H9c2 cardiomyocytes, the Fluo-3 AM molecular fluorescence probe was employed. Following treatment as described earlier, H9c2 cardiomyocytes were incubated with Fluo-3 AM at 37˚C for 30 min and washed twice with phosphate-buffered saline (PBS) to remove any extracellular dye. Subsequent to incubation for a further 30 min, the fluorescence intensity was measured on a SpectraMax M5 microplate reader (Molecular Devices, LLC, Sunnyvale, CA, USA) at an excitation wavelength of 488 nm and emission wavelength of 525 nm.

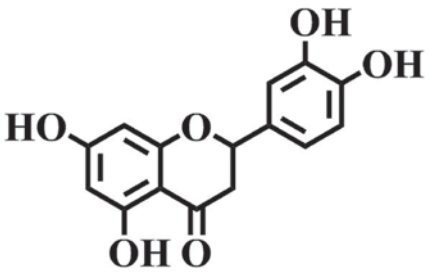

Figure 1. Chemical structure of eriodictyol.

Measurement of ROS generation. The production of intracellular ROS was detected by a fluorescence method (25) with the ROS assay kit, according to the manufacturer's protocol. Following treatment, the medium was replaced and the cells were loaded with 10 μM 2,7-dichlorodihydrofluorescein diacetate (DCFH-DA). After incubation at 37˚C for 30 min, the cells were rinsed with PBS and the fluorescence intensity was recorded on a fluorescence microplate reader at an excitation wavelength of 480 nm and emission wavelength of 525 nm.

Assessment of mitochondrial membrane potential (MMP). The fluorescent probe JC-1 was used to detect the MMP in H9c2 cardiomyocytes. In normal mitochondria, the JC-1 monomer aggregates in the matrix, whereas JC-1 maintains its monomeric form in mitochondria with reduced MMP. The fluorescence of JC-1 aggregates is measured at an excitation wavelength of 530 nm and emission wavelength of 590 nm. In the current investigation, cardiomyocytes were loaded with JC-1 (100 μM) at 37˚C for 20 min and then washed with PBS. The fluorescence intensity of the JC-1 aggregate was recorded on a fluorescence microplate reader, and the MMP was determined as the ratio of the JC-1 fluorescence intensity to that of the control group.

Opening of MPTP. The opening of MPTP was evaluated by determining the release of mitochondrial calcein, as previously described (26). Briefly, cardiomyocytes were incubated with 2 μM calcein-AM and 1 mM $CoCl_2$ at room temperature for 30 min. Next, free calcein-AM and $CoCl_2$ were washed away with Hank's balanced salt solution, and cells were incubated with $CoCl_2$ for a further 20 min at 37˚C in order to quench the fluorescence of free cytosolic calcein. The fluorescence of mitochondrial calcein in the cardiomyocytes was recorded on a fluorescence microplate reader at 490 nm for excitation and 515 nm for emission. The quenching of fluorescence in H9c2 cardiomyocytes indicated the opening of MPTP.

Level of intracellular ATP. The intercellular ATP in H9c2 cardiomyocytes was determined by the firefly luciferase method (25) with the ATP detection kit according to the manufacturer's protocol. Luciferin generates fluorescence under the catalysis of firefly luciferase, and the process consumes ATP quantitatively. The treated H9c2 cardiomyocytes were lysed on ice with 200 μl lysis reagent from the assay kit. The lysed cells were then centrifuged at 12,000 x g for 4 min at 4˚C, and 100 μl supernatant was mixed with 100 μl ATP monitoring reagent. Subsequently, the luminescence was detected on a microplate reader, and the level of intracellular ATP was derived from the standard curve.

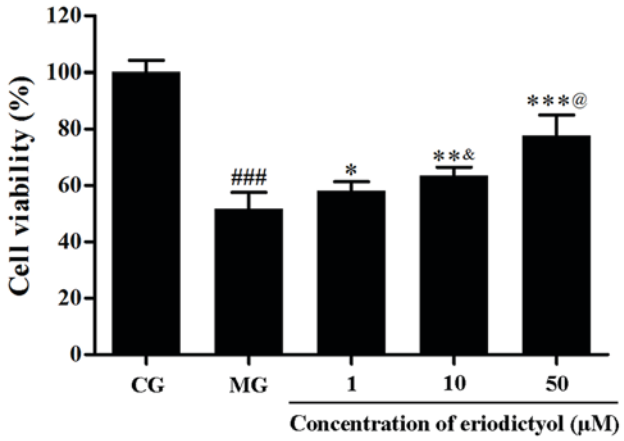

Figure 2. Effect of eriodictyol treatment (1, 10 and 50 μM) on H9c2 cardiomyocyte viability. Cell viability was determined by MTT assay (n=6). ###P<0.001 vs. the CG; *P<0.05, **P<0.01 and ***P<0.001 vs. the MG; &P<0.05 vs. the 1 μM eriodictyol; @P<0.05 vs. the 10 μM eriodictyol. CG, control group; MG, model group.

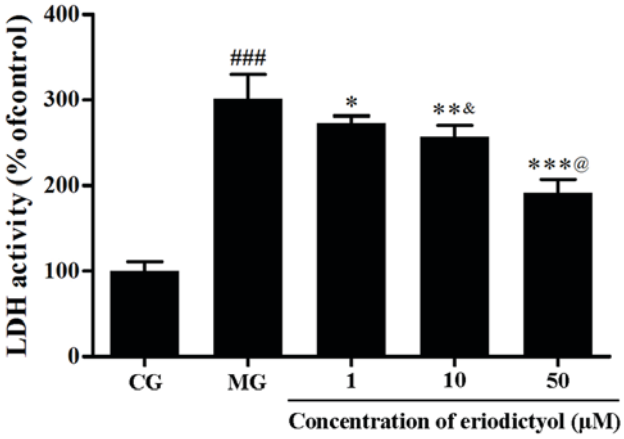

Figure 3. Effect of eriodictyol treatment (1, 10 and 50 μM) on the activity of extracellular LDH in H9c2 cardiomyocytes. n=6. ###P<0.001 vs. the CG; *P<0.05, **P<0.01 and ***P<0.001 vs. the MG; &P<0.05 vs. the 1 μM eriodictyol; @P<0.05 vs. the 10 μM eriodictyol. LDH, lactate dehydrogenase; CG, control group; MG, model group.

Caspase-3 activity. The activity of caspase-3 was quantified through a colorimetric detection kit, following the manufacturer's instructions. Briefly, subsequent to the aforementioned treatments, the H9c2 cardiomyocytes were lysed and centrifuged at 16,000 x g for 10 min at 4˚C. The supernatant was then incubated with the substrate Ac-DEVD-pNA at 37˚C for 2 h, and the absorbance was measured on a microplate reader at 405 nm. The relative caspase-3 activity was expressed as a percentage of the control group, as previous described (27).

Western blot analysis. The protein expression levels of caspase-3, Bcl-2 and Bax in pretreated H9c2 cardiomyocytes were analyzed by western blot analysis. In brief, the cells were lysed with lysis reagent containing 20 mM Tris-HCl (pH 7.4), 150 mM NaCl, 1% Triton X-100 and 1 mM phenylmethylsulfonyl fluoride on ice for 30 min. Next, the lysate was centrifuged at 12,000 x g for 15 min at 4˚C, and the supernatant was collected for the analysis of cleaved caspase-3, Bcl-2 and Bax levels. The total protein concentration in the samples was determined by BCA assay kit. Subsequently, the protein was separated by electrophoresis on a 15% SDS-polyacrylamide gel and transferred to polyvinylidene difluoride membranes. Following blocking with 5% skimmed milk at room temperature for 1 h, the membranes were incubated overnight at 4˚C with primary antibodies against cleaved caspase-3, Bcl-2, Bax and actin. The membranes were was with TBST three times, treated with the respective secondary antibodies conjugated to horseradish peroxidase (cat. no. LDAN0310; 1:1,000; Shanghai Lengton Bioscience Co., Ltd., Shanghai, China) at room temperature for 1 h and detected by an Enhanced ECL Chemiluminescent Substrate kit (cat. no. 36222ES60; Shanghai Yeasen Biotechnology Co., Ltd., Shanghai, China). Actin was used as the internal control.

Statistical analysis. All results are expressed as the means ± standard deviation. GraphPad Prism (version 5.0; GraphPad Software, Inc., La Jolla, CA, USA) was employed to analyze the results. Statistical differences between different groups were compared by one-way analysis of variance followed by Dunnett's test for multiple comparisons and Student's t-test for single comparisons. P<0.05 was considered to indicate a statistically significant difference.

Results

Effect of eriodictyol on H9c2 cardiomyocyte viability. As shown in Fig. 2, the MTT assay demonstrated that the viability of H9c2 cardiomyocytes decreased when subjected to the hypoxia/reoxygenation (P<0.001). Upon treatment with different dosages of eriodictyol, the survival of H9c2 cardiomyocytes was significantly improved and the cells viability was 77.75±7.06% of the cell viability of CG when cells were treated with 50 μM eriodictyol (P<0.001). The viability in H9c2 cardiomyocytes treated with 50 μM eriodictyol (77.75±7.06%) was significantly higher than the cells treated with 10 μM eriodictyol (63.56±2.75%; P<0.001) and the latter was significantly increased compared with the group treated with 1 μM eriodictyol (58.16±3.17%; P<0.05). These results indicate the potential cardioprotective effect of eriodictyol on H9c2 cells in a dose-dependent manner at the range of 1-50 μM eriodictyol.

Effect of eriodictyol on LDH activity. The leakage of LDH from the cytoplasm is associated with cell death. In this investigation, the activity of LDH in the culture medium of the MG (301.01±28.81%) was significantly higher as compared with that in the CG (P<0.001), which further demonstrated that the viability of H9c2 cells was affected by hypoxia/reoxygenation. When pretreated with eriodictyol, the activity of LDH in the 10 μM group with was reduced to 256.81±13.75%, which was significantly higher than the 50 μM group (191.56±13.75%; P<0.001) and lower than the 1 μM group (272.94±8.44%; P<0.05). The results indicated the release of LDH from the cytosol of H9c2 cardiomyocytes was evidently decreased in a dosage-dependent manner (Fig. 3).

Effect of eriodictyol on intracellular Ca^{2+}. To assess the intracellular Ca^{2+} content, the fluorescence probe Fluo-3 AM

was used. Following the induction of hypoxia/reoxygenation, the level of intracellular Ca^{2+} was markedly elevated to 155.28±6.13% as compared with the CG (P<0.001; Fig. 4). However, in comparison with the model group, eriodictyol reduced the overload of intracellular Ca^{2+} to 145.68±8.45, 122.41±7.64 and 102.39±8.17% upon pretreatment with 1, 10 and 50 μM, respectively (Fig. 4). These results provided evidence that eriodictyol was able to reduce the overload of intracellular Ca^{2+} in the hypoxia/reoxygenation cell model.

Effect of eriodictyol on ROS generation. The intracellular ROS generation was determined through the fluorescence intensity of DCFH-DA. The results indicated that the relative fluorescence intensity in the MG (148.84±5.16%) was significantly higher compared with that in the CG (P<0.001). By contrast, when cells were treated with eriodictyol, the fluorescence intensity was significantly decreased to 139.25±8.68% (P<0.05), 111.89±9.10 and 101.33±4.57% (both P<0.001) compared with the MG group (Fig. 5). The fluorescence intensity of 10 μM (111.89±9.10%) was lower compared with 1 μM (139.25±8.68%; P<0.05) and higher compared with 50 μM (101.33±4.57%; P<0.05). This indicated that eriodictyol was able to downregulate the generation of intracellular ROS.

Effect of eriodictyol on MMP. In order to determine the MMP in H9c2 cardiomyocytes, the fluorescent probe JC-1 was used. Compared with the CG, the fluorescence intensity in the MG (41.89±3.75%) was significantly decreased (P<0.001), which indicated the collapse of MMP in H9c2 cardiomyocytes following hypoxia/reoxygenation. However, when pretreated with 1, 10 and 50 μM eriodictyol, the fluorescence intensity was significantly elevated to 48.00±4.74% (P<0.05), 62.92±8.56 and 79.89±6.24% (both P<0.001), respectively, compared with the MG group (Fig. 6). Meanwhile, among these groups treated with eriodictyol, the 10 μM group was significantly higher than the 1 μM group lower than the 50 μM (both P<0.05). These findings revealed that the collapse of MMP in hypoxia/reoxygenation-treated H9c2 cardiomyocytes was attenuated by eriodictyol.

Effect of eriodictyol on the opening of MPTP. The MPTP opening was evaluated through the fluorescence intensity of free calcein in mitochondria. As shown in Fig. 7, under hypoxia/reoxygenation, the fluorescence intensity of mitochondrial calcein was approximately half that of the CG (50.11±6.00%; P<0.001), which demonstrated that the MPTP opened. Upon treatment with 1, 10 and 50 μM eriodictyol, the fluorescence intensity increased significantly to 58.83±6.84% (P<0.05), 63.75±8.00% (P<0.01) and 80.40±5.92% (P<0.001), respectively, compared to the MG group (Fig. 7). Compared with the CG group (100±11.83%), the ATP level in the MG group (52.62±5.87%) was significantly decreased (P<0.001). Eriodictyol (1, 10 and 50 μM) pre-treatement increased ATP levels to 59.69±4.95% (P<0.05), 69.23±3.27% (P<0.01) and 80.52±9.52% (P<0.001), respectively, compared with the MG group. These results implied that eriodictyol inhibited the MPTP opening.

Effect of eriodictyol on ATP depletion. The level of intracellular ATP represents the function of mitochondria. To detect

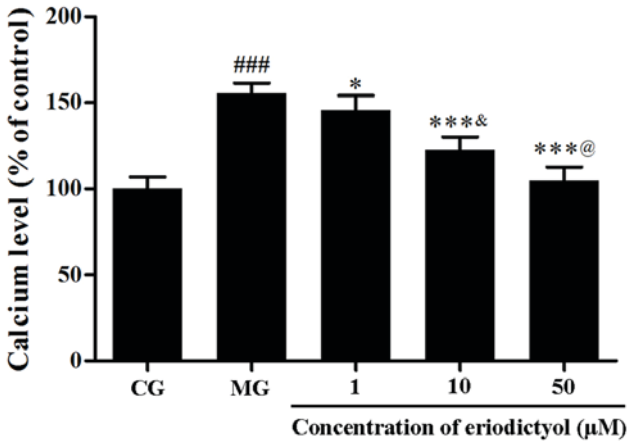

Figure 4. Effect of eriodictyol treatment (1, 10 and 50 μM) on intracellular Ca^{2+}. n=6. ###P<0.001 vs. the CG; *P<0.05 and ***P<0.001 vs. the MG; &P<0.05 vs. the 1 μM eriodictyol; @P<0.05 vs. the 10 μM eriodictyol. CG, control group; MG, model group.

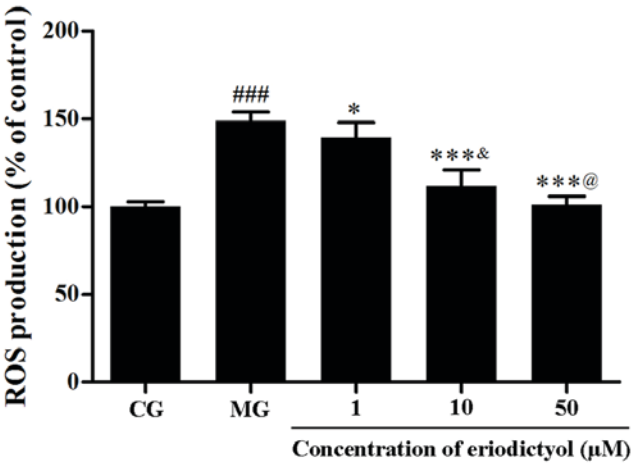

Figure 5. Effect of eriodictyol treatment (1, 10 and 50 μM) on ROS production. n=6. ###P<0.001 vs. the CG; *P<0.05 and ***P<0.001 vs. the MG; &P<0.05 vs. the 1 μM eriodictyol; @P<0.05 vs. the 10 μM eriodictyol. ROS, reactive oxygen species; CG, control group; MG, model group.

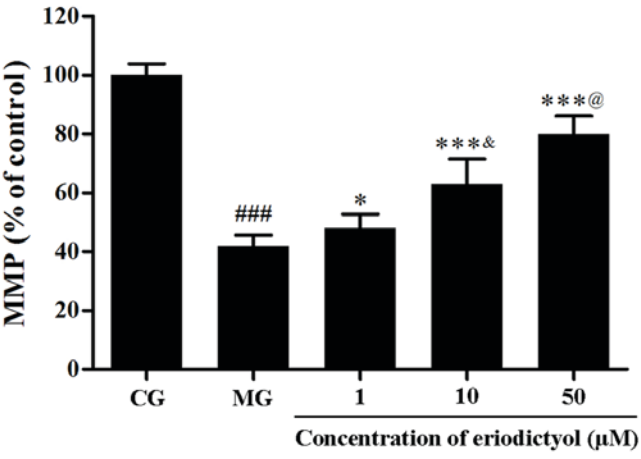

Figure 6. Effect of eriodictyol treatment (1, 10 and 50 μM) on the MMP in H9c2 cardiomyocytes. n=6. ###P<0.001 vs. the CG; *P<0.05 and ***P<0.001 vs. the MG; &P<0.05 vs. the 1 μM eriodictyol; @P<0.05 vs. the 10 μM eriodictyol. MMP, mitochondrial membrane potential; CG, control group; MG, model group.

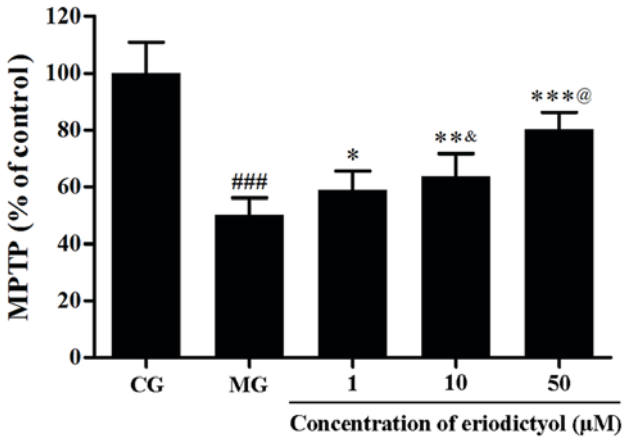

Figure 7. Effect of eriodictyol treatment (1, 10 and 50 μM) on MPTP opening. n=6. ###P<0.001 vs. the CG; *P<0.05, **P<0.01 and ***P<0.001 vs. the MG; &P<0.05 vs. the 1 μM eriodictyol; @P<0.05 vs. the 10 μM eriodictyol. MPTP, mitochondrial permeability transition pore; CG, control group; MG, model group.

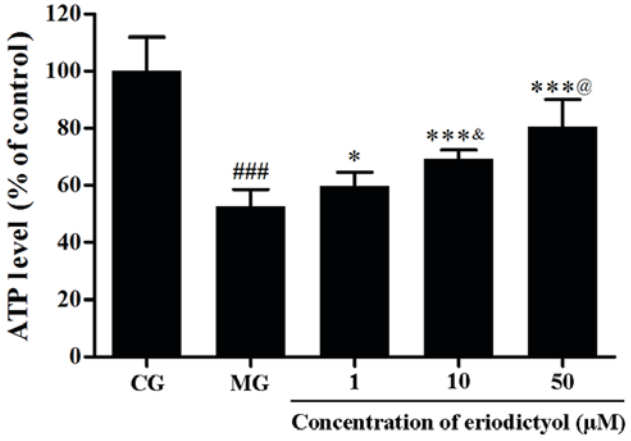

Figure 8. Effect of eriodictyol treatment (1, 10 and 50 μM) on the depletion of ATP. n=6. ###P<0.001 vs. the CG; *P<0.05 and ***P<0.001 vs. the MG; &P<0.05 vs. the 1 μM eriodictyol; @P<0.05 vs. the 10 μM eriodictyol. CG, control group; MG, model group.

the depletion of intracellular ATP, the firefly luciferase method was used. Hypoxia/reoxygenation in H9c2 cardiomyocytes resulted in the decline of the intracellular ATP level, whereas treatment with eriodictyol enhanced the ATP level. The ATP level in the 10 μM eriodictyol group was significantly higher than that in the 1 μM group as well as lower than 50 μM group (both P<0.05; Fig. 8). Compared with the CG group (100±11.83%), the ATP level in the MG group (52.62±5.87%) was significantly decreased (P<0.001). Pretreated with eriodictyol (1, 10 and 50 μM), compared with the MG group, the ATP levels were increased to 59.69±4.95% (P<0.05), 69.23±3.27% (P<0.001) and 80.52±9.52% (P<0.001), respectively. These results indicated that eriodictyol treatment was able to improve the depletion of intracellular ATP in the cardiomyocytes.

Effect of eriodictyol on caspase-3 activity and expression levels of caspase-3, Bcl-2 and Bax. As a member of the cysteinyl aspartate specific protease family, caspase-3 serves a pivotal role in apoptosis through hydrolyzed cleavage (28). Western blot analysis

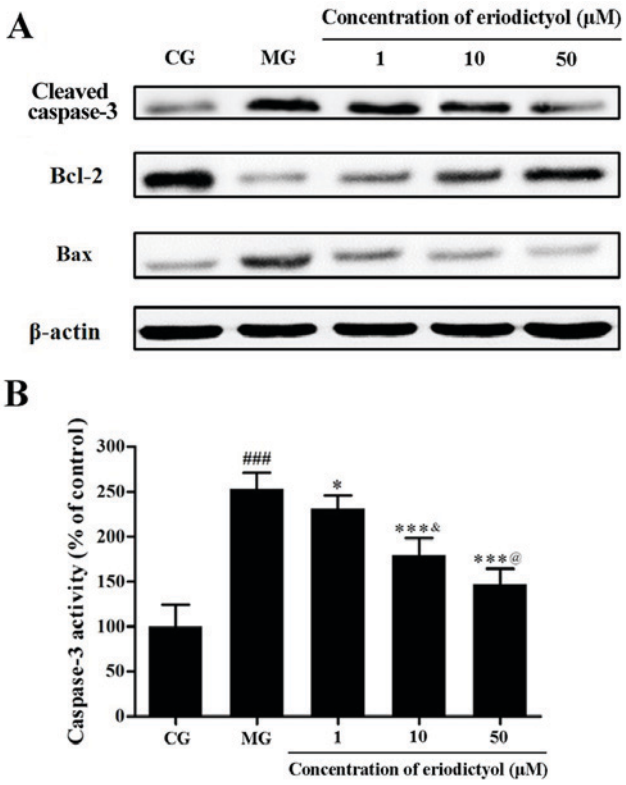

Figure 9. Effect of eriodictyol on the apoptosis of H9c2 cardiomyocytes induced by hypoxia/reoxygenation. (A) Western blot analysis of the protein expression levels of cleaved caspase-3, Bcl-2 and Bax. (B) Activity of caspase-3 in H9c2 cardiomyocytes (n=6). ###P<0.001 vs. the CG; *P<0.05 and ***P<0.001 vs. the MG; &P<0.05 vs. the 1 μM eriodictyol; @P<0.05 vs. the 10 μM eriodictyol. Bcl-2, B-cell lymphoma-2; Bax, Bcl-2-associated X protein; CG, control group; MG, model group.

revealed that hypoxia/reoxygenation promoted the expression of caspase-3 in H9c2 cardiomyocytes, while eriodictyol reduced this expression by different extents (Fig. 9A). In addition, colorimetric detection further confirmed the activity of caspase-3 quantitatively. Compared with the control group, the caspase-3 activity was markedly elevated in H9c2 cardiomyocytes treated by hypoxia/reoxygenation. However, in the presence of eriodictyol, the increased activity of caspase-3 was inhibited accordingly. Similarly, the activity of caspase-3 in the 10 μM eriodictyol group was significantly lower than that in 1 μM group as well as higher than 50 μM group (both P<0.05; Fig. 9B). The activity of caspase-3 in the MG group (253.38±17.80%) was significantly decreased compared with the CG group (100.00±24.74%; P<0.001). In contrast to the MG group, caspase-3 activity in the 1, 10 and 50 μM eriodictyol-treated groups was significantly decreased to 230.80±15.03% (P<0.05), 179.40±18.85% (P<0.001) and 147.09±17.41% (P<0.001), respectively.

Bcl-2 and Bax are the major members of the Bcl-2 protein family, which are involved in mitochondrion-mediated apoptosis. The former demonstrates an anti-apoptotic effect, whereas the latter exhibits a pro-apoptotic effect (29). In the present study, the expression of Bcl-2 was downregulated by hypoxia/reoxygenation in contrast to that in the control group. However, treatment with eriodictyol was observed to upregulate Bcl-2 expression. Accordingly, hypoxia/reoxygenation upregulated the expression of Bax, while eriodictyol treatment suppressed this increased expression (Fig. 9B).

Discussion

Myocardial ischemia and subsequent reperfusion is the major cause of myocardial infarction. The oxygen deprivation will lead to the breakdown of redox homeostasis and ROS overproduction. As the major site of ROS production, mitochondria serve an important role in the injury of myocardial ischemia and reperfusion (30). In addition to the overproduction of ROS, overload of intracellular Ca^{2+} also affects the function of the mitochondria (31). As the key determinant of mitochondrial dysfunction, the MPTP will open (32). The electrochemical gradient across the inner mitochondrial membrane (MMP) is necessary for mitochondrial function (33). Following the opening of MPTP, free solutes and proteins can be distributed across the inner mitochondrial membrane and result in the collapse of the MMP (34). The dysfunction of mitochondria also leads to the depletion of ATP due to MPTP opening (35), and finally results in the cardiomyocyte apoptosis (36).

Caspases are cysteinyl aspartate specific proteases with a central role in apoptosis, and their activation occurs through cleavage at specific sites (37). As an effector enzyme, caspase-3 is the key mediator responsible for promoting cell apoptosis (38). In addition, Bcl-2 and Bax are members of the Bcl-2 protein family that participate in mitochondrion-mediated apoptosis. Bcl-2 prevents apoptosis and blocks the activation of caspase-3, while Bax promotes cell apoptosis (39).

In the present study, mitochondrial dysfunction and cell injury induced by hypoxia/reoxygenation were observed. Pretreatment with eriodictyol increased the cell survival and blocked the leakage of LDH from the cytosol, which indicates the potential cardioprotective effect of eriodictyol. Further experiments revealed that eriodictyol improved the dysfunction of mitochondria through suppressing the overload of intracellular Ca^{2+}, preventing the overproduction of ROS, blocking the opening of MPTP, increasing the MMP level and decreasing ATP depletion. As important intracellular signaling molecules, there is interplay between Ca^{2+} and ROS production. Ca^{2+} may increase ROS production by enhancing metabolism and ROS regulates Ca^{2+} homeostasis through reciprocal redox (40). Meanwhile, the interplay between ROS and Ca^{2+} triggers the opening of MPTP opening, which leads to the collapse of MMP (41). In addition, as the main source of ATP, mitochondria may fail to synthesize enough ATP to maintain cellular function due to the dysfunction of MMP (42).

Furthermore, eriodictyol inhibited the apoptosis of H9c2 cardiomyocytes through upregulating the expression of Bcl-2 and downregulating the expression levels of Bax and caspase-3, as well as reducing the activity of caspase-3. As a bioactive flavonoid, eriodictyol showed many protective effects through the inhibition of oxidative stress (14,15,17,18). At the same time, eriodictyol and its glucoside can protect against cerebral ischemia injury *in vitro* and *in vivo* (16,43). To the best of our knowledge, the present study is the first to demonstrate the protective effects of eriodictyol on cardiomyocytes injured by hypoxia/reoxygenation, which indicates its potential application in the prevention of myocardial ischemia and reperfusion injury.

In conclusion, the results of the present study demonstrated the myocardial protective effects of eriodictyol and relevant mechanisms *in vitro*. Eriodictyol can enhance the survival of H9c2 cardiomyocytes injured by hypoxia/reoxygenation. The mechanisms involve the improvement of mitochondrial dysfunction and inhibition of apoptosis via the mitochondria-mediated signaling pathway, including the upregulation of Bcl-2, downregulation of Bax and inhibition of caspase-3. These results provided evidence for further evaluations *in vivo* for the development of novel therapeutic approaches for myocardial infarction.

References

1. Yellon DM and Hausenloy DJ: Realizing the clinical potential of ischemic preconditioning and postconditioning. Nat Clin Pract Cardiovasc Med 2: 568-575, 2005.
2. Yellon DM and Hausenloy DJ: Myocardial reperfusion injury. New Eng J Med 357: 1121-1135, 2007.
3. Hausenloy DJ and Yellon DM: Targeting myocardial reperfusion injury-the search continues. New Eng J Med 373: 1073-1075, 2015.
4. Ong SB, Samangouei P, Kalkhoran SB and Hausenloy DJ: The mitochondrial permeability transition pore and its role in myocardial ischemia reperfusion injury. J Mol Cell Cardiol 78: 23-34, 2015.
5. Hausenloya DJ, Duchenb MR and Yellon DM: Inhibiting mitochondrial permeability transition pore opening at reperfusion protects against ischaemia-reperfusion injury. Cardiovasc Res 60: 617-625, 2003.
6. Pagliaro P, Moro F, Tullio F, Perrelli MG and Penna C: Cardioprotective pathways during reperfusion: Focus on redox signaling and other modalities of cell signaling. Antioxid Redox Signal 14: 833-850, 2011.
7. Zhao GL, Yu LM, Gao WL, Duan WX, Jiang B, Liu XD, Zhang B, Liu ZH, Zhai ME, Jin ZX, *et al*: Berberine protects rat heart from ischemia/reperfusion injury via activating JAK2/STAT3 signaling and attenuating endoplasmic reticulum stress. Acta Pharmacol Sin 37: 354-367, 2016.
8. Li Q, Shen L, Wang Z, Jiang HP and Liu LX: Tanshinone IIA protects against myocardial ischemia reperfusion injury by activating the PI3K/Akt/mTOR signaling pathway. Biomed Pharmacother 84: 106-114, 2016.
9. Gao Y, Jia P, Shu W and Jia D: The protective effect of lycopene on hypoxia/reoxygenation-induced endoplasmic reticulum stress in H9C2 cardiomyocytes. Eur J Pharmacol 774: 71-79, 2016.
10. de Sousa LM, de Carvalho JL, da Silva HC, Lemos TL, Arriaga AM, Braz-Filho R, Militão GC, Silva TD, Ribeiro PR and Santiago GM: New cytotoxic bibenzyl and other constituents from *Bauhinia ungulata* L. (Fabaceae). Chem Biodivers 13: 1630-1635, 2016.
11. Milella L, Milazzo S, De Leo M, Vera Saltos MB, Faraone I, Tuccinardi T, Lapillo M, De Tommasi N and Braca A: α-Glucosidase and α-amylase inhibitors from *arcytophyllum thymifolium*. J Nat Prod 79: 2104-2112, 2016.
12. Zhong JD, Feng Y, Li HM, Xia XS and Li RT: A new flavonoid glycoside from *Elsholtzia bodinieri*. Nat Prod Res 30: 2278-2284, 2016.
13. Zeng B, Chen K, Du P, Wang SS, Ren B, Ren YL, Yan HS, Liang Y and Wu FH: Phenolic compounds from *Clinopodium chinense* (Benth.) O. Kuntze and their inhibitory effects on α-Glucosidase and vascular endothelial cells injury. Chem Biodivers 13: 596-601, 2016.
14. Lou H, Jing X, Ren D, Wei X and Zhang X: Eriodictyol protects against H_2O_2-induced neuron-like PC12 cell death through activation of Nrf2/ARE signaling pathway. Neurochem Int 61: 251-257, 2012.
15. Jing X, Shi H, Zhu X, Wei X, Ren M, Han M, Ren D and Lou H: Eriodictyol attenuates β-amyloid 25-35 peptide-induced oxidative cell death in primary cultured neurons by activation of Nrf2. Neurochem Res 40: 1463-1471, 2015.
16. Ferreira Ede O, Fernandes MY, Lima NM, Neves KR, Carmo MR, Lima FA, Fonteles AA, Menezes AP and Andrade GM: Neuroinflammatory response to experimental stroke is inhibited by eriodictyol. Behav Brain Res 312: 321-332, 2016.
17. Li CZ, Jin HH, Sun HX, Zhang ZZ, Zheng JX, Li SH and Han SH: Eriodictyol attenuates cisplatin-induced kidney injury by inhibiting oxidative stress and inflammation. Eur J Pharmacol 772: 124-130, 2016.

18. Zhu GF, Guo HJ, Huang Y, Wu CT and Zhang XF: Eriodictyol, a plant flavonoid, attenuates LPS-induced acute lung injury through its antioxidative and anti-inflammatory activity. Exp Ther Med 10: 2259-2266, 2015.
19. Lee JK: Anti-inflammatory effects of eriodictyol in lipopolysaccharide-stimulated Raw 264.7 murine macrophages. Arch Pharm Res 34: 671-679, 2011.
20. Rossato MF, Trevisan G, Walker CI, Klafke JZ, de Oliveira AP, Villarinho JG, Zanon RB, Royes LF, Athayde ML, Gomez MV and Ferreira J: Eriodictyol: A flavonoid antagonist of the TRPV1 receptor with antioxidant activity. Biochem Pharmacol 81: 544-551, 2011.
21. Habtemariam S and Dagne E: Comparative antioxidant, prooxidant and cytotoxic activity of sigmoidin A and eriodictyol. Planta Med 76: 589-594, 2010.
22. Walker J, Reichelt KV, Obst K, Widder S, Hans J, Krammer GE, Ley JP and Somoza V: Identification of an anti-inflammatory potential of Eriodictyon angustifolium compounds in human gingival fibroblasts. Food Funct 7: 3046-3055, 2016.
23. Ferreira PS, Spolidorio LC, Manthey JA and Cesar TB: Citrus flavanones prevent systemic inflammation and ameliorate oxidative stress in C57BL/6J mice fed high-fat diet. Food Funct 7: 2675-2681, 2016.
24. Chen C, He H, Luo Y, Zhou M, Yin D and He M: Involvement of Bcl-2 signal pathway in the protective effects of apigenin on anoxia/reoxygenation-induced myocardium injury. J Cardiovasc Pharmacol 67: 152-163, 2016.
25. Ji HJ, Wang DM, Hu JF, Sun MN, Li G, Li ZP, Wu DH, Liu G and Chen NH: IMM-H004, a novel courmarin derivative, protects against oxygen-and glucose-deprivation/restoration-induced apoptosis in PC12 cells. Eur J Pharmacol 723: 259-266, 2014.
26. Wang M, Sun GB, Zhang JY, Luo Y, Yu YL, Xu XD, Meng XB, Zhang MD, Lin WB and Sun XB: Elatoside C protects the heart from ischaemia/reperfusion injury through the modulation of oxidative stress and intracellular Ca^{2+} homeostasis. Int J Cardiol 185: 167-176, 2015.
27. Li JZ, Yu SY, Wu JH, Shao QR and Dong XM: Paeoniflorin protects myocardial cell from doxorubicin-induced apoptosis through inhibition of NADPH oxidase. Can J Physiol Pharmacol 90: 1569-1575, 2012.
28. Shalini S, Dorstyn L, Dawar S and Kumar S: Old, new and emerging functions of caspases. Cell Death Differ 22: 526-539, 2015.
29. Ding H, Han R, Chen X, Fang W, Liu M, Wang X, Wei Q, Kodithuwakku ND and Li Y: Clematichinenoside (AR) attenuates hypoxia/reoxygenation-induced H9c2 cardiomyocyte apoptosis via a mitochondria-mediated signaling pathway. Molecules 21: pii: E683, 2016.
30. Madungwe NB, Zilberstein NF, Feng Y and Bopassa JC: Critical role of mitochondrial ROS is dependent on their site of production on the electron transport chain in ischemic heart. Am J Cardiovasc Dis 6: 93-108, 2016.
31. Hurst S, Hoek J and Sheu SS: Mitochondrial Ca^{2+} and regulation of the permeability transition pore. J Bioenerg Biomembr 49: 27-47, 2017.
32. Weiss JN, Korge P, Honda HM and Ping P: Role of the mitochondrial permeability transition in myocardial disease. Circ Res 93: 292-301, 2003.
33. Marchetti P, Castedo M, Susin SA, Zamzami N, Hirsch T, Macho A, Haeffner A, Hirsch F, Geuskens M and Kroemer G: Mitochondrial permeability transition is a central coordinating event of apoptosis. J Exp Med 184: 1155-1160, 1996.
34. Kroemer G: Mitochondrial control of apoptosis: An overview. Biochem Soc Symp 66: 1-15, 1999.
35. Li YY, Xiao L, Qiu LY, Yan YF, Wang H, Duan GL, Liao ZP and Chen HP: Sasanquasaponin-induced cardioprotection involves inhibition of mPTP opening via attenuating intracellular chloride accumulation. Fitoterapia 116: 1-9, 2017.
36. Whelan RS, Kaplinskiy V and Kitsis RN: Cell death in the pathogenesis of heart disease: Mechanisms and significance. Annu Rev Physiol 72: 19-44, 2010.
37. Budihardjo I, Oliver H, Lutter M, Luo X and Wang X: Biochemical pathways of caspase activation during apoptosis. Annu Rev Cell Dev Biol 15: 269-290, 1999.
38. Uchiyama T, Otani H, Okada T, Ninomiya H, Kido M, Imamura H, Nogi S and Kobayashi Y: Nitric oxide induces caspase-dependent apoptosis and necrosis in neonatal rat cardiomyocytes. J Mol Cell Cardiol 34: 1049-1061, 2002.
39. Youle RJ and Strasser A: The Bcl-2 protein family: Opposing activities that mediate cell death. Nat Rev Mol Cell Biol 9: 47-59, 2008.
40. Yan Y, Wei CL, Zhang WR, Cheng HP and Liu J: Cross-talk between calcium and reactive oxygen species signaling. Acta Pharmacol Sin 27: 821-826, 2006.
41. Görlach A, Bertram K, Hudecova S and Krizanova O: Calcium and ROS: A mutual interplay. Redox Biol 6: 260-271, 2015.
42. Jašová M, Kancirová I, Waczulíková I and Ferko M: Mitochondria as a target of cardioprotection in models of preconditioning. J Bioenerg Biomembr 49: 357-368, 2017.
43. Jing X, Ren D, Wei X, Shi H, Zhang X, Perez RG, Lou H and Lou H: Toxicol Appl Pharmacol 273: 672-679, 2013.